THE GEOLOGICAL SOCIETY OF AMERICA®

Geospatial analysis of Oklahoma (USA) earthquakes (2011–2016): Quantifying the limits of regional-scale earthquake mitigation measures

Ryan M. Pollyea[1], Neda Mohammadi[2], John E. Taylor[2], and Martin C. Chapman[1]
[1]Department of Geosciences, Virginia Polytechnic Institute and State University, 926 West Campus Drive, Blacksburg, Virginia 24061, USA
[2]School of Civil and Environmental Engineering, Georgia Institute of Technology, 790 Atlantic Drive NW, Atlanta, Georgia 30332, USA

ABSTRACT

The annual earthquake rate in Oklahoma (United States) has increased dramatically in recent years, owing in large part to the rapid proliferation of salt-water disposal (SWD) wells associated with unconventional oil and gas recovery. This study presents a geospatial analysis of earthquake occurrence and SWD volume within a 68,420 km² area in north-central Oklahoma between 2011 and 2016. Results indicate that (1) the annual geographic centroid of Arbuckle Group SWD well locations predicts the geographic centroid for M3.0+ earthquake occurrence within an ~1σ radius of gyration when the well centroid is geometrically weighted by SWD volume; (2) between 2014 and 2016 Arbuckle SWD volume and earthquake occurrence are spatially cross-correlated to a length scale of 125 km; and (3) earthquake mitigation strategies implemented in late 2015 and 2016 are preferentially affecting the joint variability of SWD volume and small-magnitude earthquakes. These results suggest that current earthquake mitigation may require further volume reductions and/or greater areal extent to increase effectiveness.

INTRODUCTION

Between 1960 and 2008, Oklahoma (United States) experienced ~1 M3.0+ earthquake per year (Ellsworth, 2013); however, this earthquake recurrence rate increased sharply to >1 M3.0+ earthquake per day between 2011 and 2016 (Fig. 1). This dramatic increase in earthquake frequency occurred contemporaneously with the rapid proliferation of both unconventional oil and gas recovery and class II underground injection control (UIC) wells; the latter are used to dispose of highly brackish water produced during oil and gas recovery (Walsh and Zoback, 2015; Weingarten et al., 2015). Earthquake swarms in Oklahoma have been located at depths between 4 and 8 km (Walsh and Zoback, 2015; McNamara et al., 2015a) and have been shown to be collocated with high-volume salt-water disposal (SWD) wells in the Arbuckle Group (Keranen et al., 2014). As a result, there is general consensus that SWD in Arbuckle reservoirs is triggering earthquakes in the underlying crystalline basement rock (Ellsworth, 2013; Keranen et al., 2013, 2014; Weingarten et al., 2015). These fluid-triggered earthquakes have transformed Oklahoma from a low-seismicity state to the most seismically active state in the conterminous United States, causing profound changes in Oklahoma's earthquake hazard forecast (Petersen et al., 2016, 2017) and regulatory environment (Baker, 2015; OCC, 2015a, 2015b, 2016a, 2016b, 2016c).

In April 2015, the Oklahoma Geological Survey (OGS) released a memo acknowledging that "OGS considers it very likely that the majority of recent earthquakes, particularly those in central and north-central Oklahoma, are triggered by the injection of produced water in disposal wells" (Andrews and Holland, 2015, p. 1). Consequently, the Oklahoma Corporation Commission, which regulates oil and gas development in Oklahoma, began implementing earthquake mitigation directives, including (1) weekly reporting requirements for injection volume and wellhead pressure in Arbuckle disposal wells; (2) mechanical integrity tests for wells injecting 20,000 or more barrels per day (OCC, 2015a); and (3) targeted injection volume reductions within 4.8, 9.6, and 16 km buffer zones around earthquake swarms (OCC, 2015b). The slight decrease in earthquake occurrence starting in 2016 (Fig. 1) has been attributed to those mitigation efforts; however, decreasing SWD volume may have also been a result of rapidly decreasing oil prices beginning in August 2014. Nevertheless, media outlets reported resistance from the oil and gas industry to the directives of the Oklahoma Corporation Commission, which lacked statutory authority under the Oklahoma Administrative Code (e.g., see Mack et al., 2016). In response, Oklahoma Governor Mary Fallin signed House Bill HB3158 into law on 18 April 2016, giving the Oklahoma Corporation Commission exclusive jurisdiction, power, and authority over UIC class II injection wells in Oklahoma, as well as a mechanism to implement emergency SWD volume reductions.

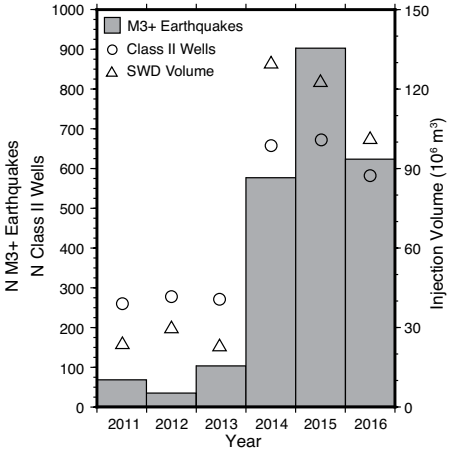

Figure 1. Total number of M3.0+ earthquakes, class II injection wells, and salt-water disposal (SWD) volume within the study area. Data were acquired by Internet download from the Oklahoma Geological Survey and Oklahoma Corporation Commission websites, respectively (data sources are found in the Data Repository [see footnote 1]).

Despite the earthquake mitigation efforts in 2015 and 2016, two noteworthy earthquakes occurred in the latter half of 2016. On 3 September 2016, an M5.8 earthquake occurred near Pawnee, Oklahoma, and is the largest recorded earthquake in Oklahoma history (Yeck et al., 2017). The Pawnee earthquake resulted in sufficient infrastructure damage (Clayton et al., 2016) for Governor Fallin to declare a state of emergency for Pawnee County. On 7 November 2016, an M5.0 earthquake occurred near Cushing, Oklahoma, home to the largest oil storage facility in the United States; at the time of this writing it holds 62×10^6 barrels (bbl) of oil valued at approximately US$2.8 B (assuming $45/bbl) (U.S. Energy Information Administration, 2017), thus making Cushing an area of U.S. strategic infrastructure (McNamara et al., 2015b). Following the Pawnee and Cushing earthquakes, the Oklahoma Corporation Commission exercised its statutory authority by ordering (1) all Arbuckle SWD wells within a 9.6 km radius of the epicenters to cease injections; (2) all Arbuckle SWD wells within a 16 km radius of the epicenters to reduce injection volume by 25% of the most

GSA Data Repository item 2018052 | https://doi.org/10.1130/G39945.1

recent 30 day average; and (3) all Arbuckle SWD wells within a 24 km radius of the epicenters to maintain injection volumes at or below the most recent 30 day average (OCC, 2016a, 2016b). Despite these SWD volume reductions, there were more than 600 M3.0+ earthquakes in Oklahoma in 2016, and, as a result, there remains uncertainty in the efficacy of Oklahoma Corporation Commission earthquake mitigation directives, particularly in the context of the length scales (9.6 km, 16 km, and 24 km radial distance from epicenters) required for SWD volume reductions. In addressing this uncertainty, our study implements geostatistical methods to interrogate annual changes in the spatial variability and joint variability of earthquake epicenters and SWD wastewater injection volume within Arbuckle injection wells from 2011 to 2016.

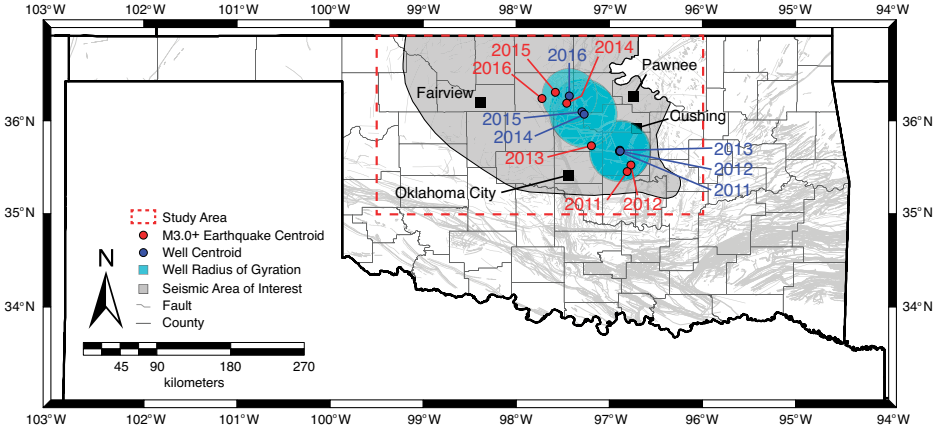

Figure 2. Annual geographic centroid locations for the years 2011–2016 (the underlying fault map is by Marsh and Holland, 2016), including volume-weighted well centroids, the 1σ radius of gyration, and M3+ earthquake centroids.

METHODS

The study area comprises a 68,420 km^2 area in north-central Oklahoma from 99.5°W to 96.0°W and 35.0°N to 37.0°N, which includes the Expanded Area of Interest for Triggered Earthquakes delineated on 7 March 2016 (OCC, 2016c) (Fig. 2). Data for earthquake occurrence and SWD volume were acquired by Internet download from the Oklahoma Geological Survey and Oklahoma Corporation Commission websites, respectively (see the GSA Data Repository[1] for details on data sources and preparation). To evaluate the spatiotemporal evolution of regional-scale M3.0+ earthquake occurrence, the time-dependent geographic centroid, $\vec{p}_e(t)$, is calculated for 1 yr time intervals between 2011 and 2016 as

$$\vec{p}_e(t) = \frac{1}{N}\sum_{i=1}^{N}\vec{p}_i, \quad (1)$$

where $\vec{p}_i$ is the location vector of each earthquake epicenter within 1 yr (t) increments, and N is the total number of earthquakes (Mohammadi et al., 2017). Similarly, the annual geographic centroid for class II injection wells, $\vec{p}_w(t)$, is calculated as

$$\vec{p}_w(t) = \frac{1}{N}\sum_{j=1}^{N}\omega_j\vec{p}_j, \quad (2)$$

where $\vec{p}_j$ is a well location, ω_j is the weighting function, and N is the total number of class II injection wells. To account for the orders-of-magnitude variability in SWD volume between wells, ω_j scales the contribution of each well location ($\vec{p}_j$) by the corresponding geometric mean contribution of SWD volume (V_j). The geometric weighting function was selected because the SWD volumes are log normally distributed for each year of the study (Fig. DR3 in the Data Repository). As a result, ω_j is calculated as

$$\omega_j = \frac{\ln V_j}{\sum_{j=1}^{N}\ln V_j}. \quad (3)$$

The variability about each well centroid is quantified on the basis of a radius of gyration (r_g), which is one standard deviation of the distance between each centroid and its underlying data,

$$r_g = \sqrt{\sum\left(\vec{p}_w - \vec{p}_j\right)^2 / N}.$$

In order to quantify the spatial covariation between SWD volume and the number of earthquakes, the experimental cross semivariogram (γ_{ij}) is calculated for each year of the study (2011–2016). The cross semivariogram quantifies spatial covariation between collocated attributes as function of separation distance under the assumption of stationarity, which simply states that attributes are grouped on the basis of the process responsible for their occurrence (Deutsch, 2002). The experimental cross semivariogram (γ_{ij}) is defined mathematically as

$$\gamma_{ij} = \frac{1}{2N(\vec{h})}\sum_{\alpha=1}^{N}\left\{\left[z_i(\vec{u}_\alpha) - z_i(\vec{u}_\alpha + \vec{h})\right]\left[z_j(\vec{u}_\alpha) - z_j(\vec{u}_\alpha + \vec{h})\right]\right\}, \quad (4)$$

where z_i and z_j are measurable attributes cosampled at position $\vec{u}_\alpha$, $\vec{h}$ is a spatial lag class (separation vector between sample locations), and N is the number of two-point comparisons (data pairs) within each lag class (Deutsch, 2002, p. 139–147). The experimental cross semivariogram returns a bulk measure of dissimilarity between cosampled attributes as a function of separation distance. Consequently, the cross semivariogram provides an indication of the strength of spatial cross-correlation between SWD volume and earthquake count. For this analysis lower γ_{ij} values indicate stronger spatial correlation (less average dissimilarity between data pairs). Moreover, the plot of γ_{ij} as a function of separation distance $\vec{h}$ reveals the length scale of cross-correlation, which is the maximum distance at which γ_{ij} remains below the covariance (sill) of the data.

Annual cross semivariograms are calculated for four earthquake magnitude thresholds: the complete earthquake catalog (M_{comp}), M3.0+, M3.5+, and M4.0+. In doing so, the study area is subdivided into a regular Cartesian grid comprising 9.6 × 9.6 km grid cells. This discretization interval is equivalent to the smallest radius for which injection operations were ceased following the 2016 earthquakes in Pawnee and Cushing, and as a result allows for cross semivariogram calculations at length scales comparable to and greater than the Oklahoma Corporation Commission post-earthquake emergency actions. Within each grid cell, the number of earthquakes and SWD volume are summed for each annual dataset, and each sum is assigned to the grid cell center coordinate, resulting in six data sets comprising grid-centered SWD volume and earthquake count for each year between 2011 and 2016. Prior to calculating the experimental cross semivariograms, the measured attributes in each annual dataset are standardized to zero mean and a variance of one (Deutsch, 2002, p. 143). Subsequently, the annual cross semivariogram calculations are post-processed by normalizing each value over its respective covariance to facilitate annual comparison of the cross-correlation structure. The GSLIB (Geostatistical Software Library) software routines nscore and gamv (Deutsch and Journel, 1998) were utilized for the standardization and cross semivariogram calculations, respectively; the latter implemented an isotropic search pattern, lag separation distance of 25 km, and lag tolerance of 12.5 km.

RESULTS AND DISCUSSION

To assess the aggregate, regional-scale spatiotemporal relationship between SWD and earthquake occurrence, Figure 2 presents the annual (2011–2016) centroid calculations for

[1]GSA Data Repository item 2018052, additional information about data sources and preparation, is available online at http://www.geosociety.org/datarepository/2018/, or on request from editing@geosociety.org.

M3.0+ earthquake epicenters (Equation 1) and volume-weighted well locations (Equation 2). In general, both the volume-weighted well centroids ($\vec{p}_w$) and earthquake centroids ($\vec{p}_e$) migrate northwest through the study area. This result is consistent with the general tendency of SWD wells to increase in number and injection volume to the northwest of the study area between 2011 and 2016 (Fig. DR4). These calculations also show that the M3.0+ earthquake centroid is within the volume-weighted well radius of gyration (r_g) for each year of the study (Fig. 2). Although centroid calculations are abstract representations of complex point processes across the study area, the consistency of these results suggests that $\vec{p}_w$ calculations anticipate $\vec{p}_e$ within a 1σ radius of gyration. Interestingly, the triggering front concept may provide a physical basis to explain the spatial relationship between $\vec{p}_w$ and $\vec{p}_e$. A triggering front (r_t) represents the maximum radial distance from an injection well to its corresponding fluid pressure perturbation. For an isotropic homogeneous reservoir, r_t is described mathematically as $r_t = \sqrt{4\pi Dt}$, where D is the hydraulic diffusivity (Shapiro and Dinske, 2009). This space-time scaling is a well-known property of diffusion, and falls out of the similarity solution for the transient diffusion equation with boundaries approximating a subsurface fluid injection (Fairley, 2016). For Arbuckle Group hydraulic diffusivity ranging between 0.5 and 4 $m^2\ s^{-1}$ (Morgan and Murray, 2015), the 1 yr r_t for a single injector ranges between 14 and 40 km, which is comparable with the annual $\vec{p}_w - \vec{p}_e$ separation distances of 17–39 km (Table 1). In aggregate, this result suggests that volume-weighted well centroid locations are a reasonable first-order predictor of regional-scale M3.0+ earthquake activity. Moreover, results of this analysis are congruent with pressure diffusion scaling, and may be a useful tool for testing the regional-scale effects of increasing or decreasing SWD volume within a geographic location.

Although the correlation between earthquake occurrence and SWD volume is reasonably explained by effective stress theory and supported by numerous field and modeling studies (Ellsworth, 2013; Keranen et al., 2014; Walsh and Zoback, 2015; Weingarten et al., 2015), there remains uncertainty in how this correlation varies with time and over what spatial scales. To analyze this uncertainty, Figure 3 presents experimental cross semivariograms (γ_{ij}) comparing SWD volume and earthquake count for each year of the study (Equation 4) using four thresholds for earthquake magnitude: M_{comp}, M3.0+, M3.5+, and M4.0+. The initial results are that the correlation coefficients between SWD volume and earthquake occurrence are positive for each year of the study, indicating that SWD volume and earthquake occurrence vary together (Table 1). These results agree with previous studies linking seismicity to SWD injection on the basis of groundwater modeling (Keranen et al., 2014), time-series analysis (Walsh and Zoback, 2015; Weingarten et al., 2015), and magnitude exceedance modeling (Langenbruch and Zoback, 2016); however, the spatial attributes of this correlation reveal interesting patterns.

Between 2011 and 2013, γ_{ij} generally oscillates about the sill (covariance) for all earthquake magnitude thresholds (Fig. 3), which suggests that while SWD volume and earthquake count are positively correlated, this relationship is not spatially correlated (i.e., the overall correlation is independent of distance). In contrast, between 2014 and 2016, the γ_{ij} values for M_{comp}, M3.0+, and M3.5+ earthquake thresholds are consistently below the sill for lag distances <125 km. This result indicates that SWD volume and earthquake count (M_{comp}, M3.0+, and M3.5+) are spatially cross-correlated, which means that regions with high SWD volume and earthquake count are more likely to be near one another (Figs. 3A–3C). Moreover, the strength of spatial cross-correlation decreases for the M3.5+ threshold (Fig. 3C), while SWD and M4.0+ earthquakes exhibit no spatial cross-correlation (Fig. 3D). For the M_{comp}, M3.0+, and M3.5+ thresholds, the cross semivariograms for 2014–2016 indicate that SWD volume and earthquake count exhibit maximum spatial correlation (lowest γ_{ij}) at lag distances of 25 km (Figs. 3A–3C), equivalent to the maximum radial distance (24 km) within which the Oklahoma Corporation Commission ordered emergency volume reductions in 2016. In addition, the effects of 2016 SWD volume reductions are apparent by comparing the 2015 and 2016 γ_{ij} values for the M_{comp} threshold (Fig. 3A); this shows that the spatial correlation between SWD volume and earthquake occurrence weakened in 2016. Interestingly, Figure 1 suggests that decreasing SWD volume in 2016 resulted in fewer M3.0+ earthquakes; however, Figure 3B indicates that the spatial cross-correlation between SWD volume and M3.0+ earthquake occurrence is unchanged between 2015 and 2016 despite SWD volume reductions. Consequently, these results suggest that Oklahoma Corporation Commission mitigation measures are preferentially decoupling the spatial cross-correlation between SWD volume and earthquake occurrence for small-magnitude earthquakes (Fig. 3A).

Between 2014 and 2016, the spatial cross-correlation for M_{comp} and M3.0+ thresholds is persistent at length scales to 125 km, suggesting that widespread SWD injections may be causing regional-scale fluid pressure accumulation within the Arbuckle Group and underlying basement rock. The consequence of regional fluid pressure accumulation is a corresponding decrease in the regional-scale effective stresses, thus further driving optimally aligned faults closer to failure. The 125 km cross-correlation range is also congruent with the 100–150 km

TABLE 1. GEOGRAPHIC CENTROIDS AND CORRELATION COEFFICIENT

Year	r_g (km)	$\vec{p}_e - \vec{p}_w$ (km)	$\rho_{NEQ, SWD}$
2011	36	26	0.81
2012	37	21	0.82
2013	37	29	0.76
2014	40	17	0.78
2015	40	39	0.76
2016	34	27	0.80

Note: r_g is the volume-weighted well radius of gyration; $\vec{p}_e - \vec{p}_w$ is the separation distance between M3.0+ earthquake and well centroids; $\rho_{NEQ, SWD}$ is the correlation coefficient between number of earthquakes (NEQ) in M_{comp} data set and salt-water disposal (SWD) volume.

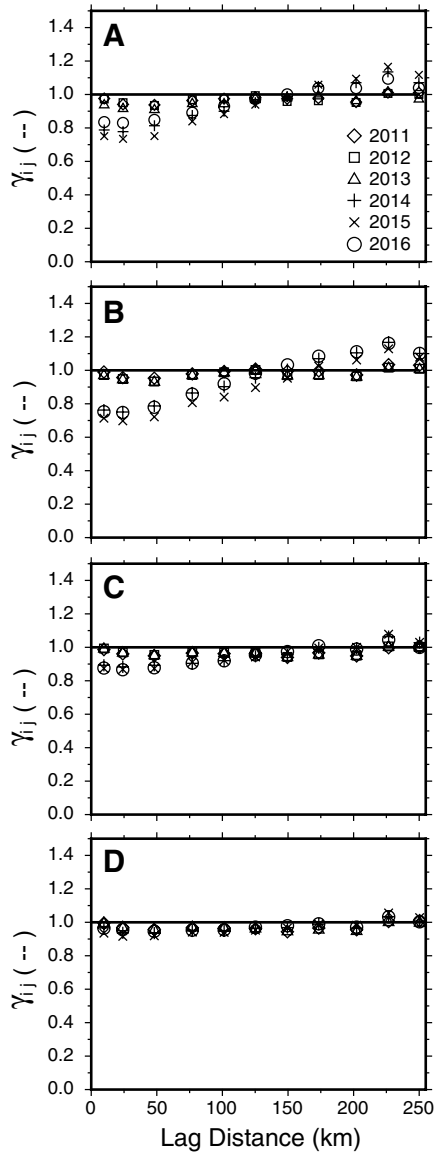

Figure 3. Annual cross semivariogram (γ_{ij}) for salt-water disposal injection volume and number of earthquakes within the study using four earthquake magnitude thresholds. A: The complete earthquake catalog (M_{comp}). B: M3+. C: M3.5+. D: M4+. Symbols represent annual calculations. Each cross semivariogram is normalized over its respective covariance resulting in a sill at γ_{ij} = 1 (solid black line).

length scale for remote triggering suggested by Huc and Main (2003). In this context, seismic wave propagation may alter the preexisting stress field along faults already approaching failure due to localized fluid pressure accumulation. Although our study cannot distinguish between the causal mechanisms (widespread fluid pressure accumulation or remote triggering), both mechanisms imply that earthquake occurrence is likely affected by SWD injections at length scales beyond the range of emergency volume reductions, as suggested by the 125 km cross-correlation structure.

CONCLUSIONS

Results from this study indicate that (1) the annual geographic centroid of Arbuckle Group SWD well locations predicts the geographic centroid for M3.0+ earthquake occurrence within an ~1σ radius of gyration when the well centroid is geometrically weighted by SWD volume; (2) Arbuckle Group injection volume and earthquake occurrence between 2014 and 2016 are spatially cross-correlated to a length scale of 125 km; and (3) earthquake mitigation strategies implemented in late 2015 and 2016 are preferentially affecting the joint variability of SWD volume and small-magnitude earthquakes, while larger magnitude earthquakes (M3.0+) appear unaffected. As a result, earthquake mitigation strategies may require further volume reductions and/or greater areal extent to increase effectiveness; however, further research is warranted to understand how time lag may affect interpretations of mitigation efficacy. The geospatial methods invoked here aggregate the outcomes of numerous complex and interdependent point processes into system-wide averages, and as a result this approach is not suitable for analyzing or testing outcomes for individual sequences of earthquakes. Nevertheless, these methods may be useful for testing the regional-scale effects of increasing or decreasing SWD volume in the context of fluid-triggered earthquake management, mitigation, and/or injection well permitting.

ACKNOWLEDGMENTS

We thank Art McGarr, Ian Main, and an anonymous reviewer for their thoughtful reviews of this study. This work received support from National Science Foundation grant 1142379 (Taylor), the School of Civil and Environmental Engineering at Georgia Institute of Technology (Mohammadi), and the Department of Geosciences at Virginia Tech (Pollyea and Chapman).

REFERENCES CITED

Andrews, R.S. and Holland, A., 2015, Statement on Oklahoma seismicity, April 21, 2015: Oklahoma Geological Survey, http://wichita.ogs.ou.edu/documents/OGS_Statement-Earthquakes-4-21-15.pdf, accessed 15 June 2017.

Baker, T., 2015, Wells located within area of interest for induced seismicity, letter dated 14 July 2015: Oklahoma Corporation Commission, http://earthquakes.ok.gov/wp-content/uploads/2015/04/Letter_to_Operators.pdf, accessed 15 June 2017.

Clayton, P., Zalachoris, G., Rathje, E., Bheemasetti, T., Caballero, S., Yu, X., and Bennett, S., 2016, The geotechnical aspects of the September 3, 2016 M5.8 Pawnee, Oklahoma earthquake: Geotechnical Extreme Events Reconnaissance (GEER) report, 14 p., http://www.geerassociation.org/administrator/components/com_geer_reports/geerfiles/Pawnee-GEERreport-FINAL_v1.2.pdf, accessed 1 November 2016.

Deutsch, C.V., 2002, Geostatistical reservoir modeling: New York, Oxford University Press, 384 p.

Deutsch, C.V., and Journel, A.G., 1998, GSLIB: Geostatistical software library and user's guide (second edition): New York, Oxford University Press, 369 p.

Ellsworth, W.L., 2013, Injection-induced earthquakes: Science, v. 341, 6142, https://doi.org/10.1126/science.1225942.

Fairley, J., 2016, Models and modeling: An introduction for Earth and environmental scientists: Chichester, UK, John Wiley & Sons, 264 p., https://doi.org/10.1002/9781119310396.

Huc, M., and Main, I.G., 2003, Anomalous stress diffusion in earthquake triggering: Correlation length, time dependence, and directionality: Journal of Geophysical Research, v. 108, 2324, https://doi.org/10.1029/2001JB001645.

Keranen, K.M., Savage, H.M., Abers, G.A., and Cochran, E.S., 2013, Potentially induced earthquakes in Oklahoma, USA: Links between wastewater injection and the 2011 Mw 5.7 earthquake sequence: Geology, v. 41, p. 699–702, https://doi.org/10.1130/G34045.1.

Keranen, K.M., Weingarten, M., Abers, G.A., Bekins, B.A., and Ge, S., 2014, Sharp increase in central Oklahoma seismicity since 2008 induced by massive wastewater injection: Science, v. 345, p. 448–451, https://doi.org/10.1126/science.1255802.

Langenbruch, C., and Zoback, M.D., 2016, How will induced seismicity in Oklahoma respond to decreased saltwater injection rates?: Science Advances, v. 2, e1601542, https://doi.org/10.1126/sciadv.1601542.

Mack, J., Handy, A., Barrett, J., and Jones, K., 2016, Seismicity triggering more regulation: Oil & Gas Financial Journal, 11 July 2016, http://www.ogfj.com/articles/print/volume-13/issue-7/features/seismicity-triggering-more-regulation.html, accessed 17 July 2017.

Marsh, S., and Holland, A., 2016, Comprehensive fault database and interpretive fault map of Oklahoma: Oklahoma Geological Survey Open-File Report OF2-2016, 15 p.

McNamara, D.E., Benz, H.M., Herrmann, R.B., Bergman, E.A., Earle, P., Holland, A., Baldwin, R., and Gassner, A., 2015a, Earthquake hypocenters and focal mechanisms in central Oklahoma reveal a complex system of reactivated subsurface strike-slip faulting: Geophysical Research Letters, v. 42, p. 2742–2749, https://doi.org/10.1002/2014GL062730.

McNamara, D.E., et al., 2015b, Reactivated faulting near Cushing, Oklahoma: Increased potential for a triggered earthquake in an area of United States strategic infrastructure: Geophysical Research Letters, v. 42, p. 8328–8332, https://doi.org/10.1002/2015GL064669.

Mohammadi, N., Taylor, J.E., and Pollyea, R.M., 2017, Spatiotemporal dynamics of public response to human-induced seismic perturbations: Proceedings of the 14th International Conference on Information Systems for Crisis Response and Management (ISCRAM), p. 666–672.

Morgan, C.B., and Murray, K.E., 2015, Characterizing small-scale permeability of the Arbuckle Group, Oklahoma: Oklahoma Geological Survey Open-File Report OF2-2015, 12 p.

OCC (Oklahoma Corporation Commission), Oklahoma Corporation Commission (OCC) announces next steps in continuing response to earthquake concerns, 17 July 2015: http://occeweb.com/News/DIRECTIVE-2.pdf, accessed 15 June 2017.

OCC (Oklahoma Corporation Commission), 2015b, Reduction in volumes for wells located in area of interest for induced seismicity: http://earthquakes.ok.gov/wp-content/uploads/2015/04/Cushing_10-16-15LetterSeismicity_All_Final.pdf, accessed 15 July 2017.

OCC (Oklahoma Corporation Commission), 2016a, Advisory—Pawnee, 3 November 2016: http://www.occeweb.com/News/2016/11-03-16PAWNEE%20POSTING.pdf, accessed 15 June 2017.

OCC (Oklahoma Corporation Commission), 2016b, Advisory 4—Cushing, 8 November 2016: https://www.occeweb.com/News/2016/11-08-16CUSHING%20PLAN.pdf, accessed 15 June 2017.

OCC (Oklahoma Corporation Commission), 2016c, Media advisory—Regional earthquake response plan for central Oklahoma and expansion of area of interest, 7 March 2016: http://www.occeweb.com/News/2016/03-07-16ADVISORY-AOI%2C%20VOLUME%20REDUCTION.pdf, accessed 1 July 2017.

Petersen, M.D., Mueller, C.S., Moschetti, M.P., Hoover, S.M., Llenos, A.L., Ellsworth, W.L., Michael, A.J., Rubinstein, J.L., McGarr, A.F., and Rukstales, K.S., 2016, One-year seismic hazard forecast for the central and eastern United States from induced and natural earthquakes: U.S. Geological Survey Open-File Report 2016-1035, 52 p., https://doi.org/10.3133/ofr20161035.

Petersen, M.D., et al., 2017, One-year seismic-hazard forecast for the central and eastern United States from induced and natural earthquakes: Seismological Research Letters, v. 88, p. 772–783, https://doi.org/10.1785/0220170005.

Shapiro, S., and Dinske, C., 2009, Scaling of seismicity induced by nonlinear fluid-rock interaction: Journal of Geophysical Research, v. 114, B09307, https://doi.org/10.1029/2008JB006145.

U.S. Energy Information Administration, 2017, U.S. Energy Information Administration (EIA) Weekly Cushing, OK, ending stocks excluding SPR of crude oil: https://www.eia.gov/dnav/pet/hist/LeafHandler.ashx?n=PET&s=W_EPC0_SAX_YCUOK_MBBL&f=W, accessed 15 June 2017.

Walsh, F.R., and Zoback, M.D., 2015, Oklahoma's recent earthquakes and saltwater disposal: Science Advances, v. 1, e1500195, https://doi.org/10.1126/sciadv.1500195.

Weingarten, M., Ge, S., Godt, J.W., Bekins, B.A., and Rubinstein, J.L., 2015, High-rate injection is associated with the increase in US mid-continent seismicity: Science, v. 348, p. 1336–1340, https://doi.org/10.1126/science.aab1345.

Yeck, W., Hayes, G., McNamara, D., Rubinstein, J., Barnhart, W., Earle, P., and Benz, H., 2017, Oklahoma experiences largest earthquake during ongoing regional wastewater injection hazard mitigation efforts: Geophysical Research Letters, v. 44, p. 711–717, https://doi.org/10.1002/2016GL071685.

Manuscript received 11 September 2017
Revised manuscript received 29 November 2017
Manuscript accepted 30 November 2017

Printed in USA